

A Routing Method with Link Information-based Rule Selection in Non-Terrestrial Networks

Tomohiro Korikawa, Chikako Takasaki, Kyota Hattori, and Hidenari Oowada

Network Service Systems Laboratories, NTT Corporation, Tokyo, Japan

E-mail: {tomohiro.koorikawa.xa, chikako.takasaki.dp, kyota.hattori.vj, hidenari.oowada.uk}@hco.ntt.co.jp

Abstract—Non-terrestrial networks (NTN) are a promising approach in beyond 5G/6G era to provide ubiquitous connectivity to everywhere, including uncovered or underserved areas. NTN enables covering wide areas from the sky by employing satellites and unmanned aerial vehicles (UAVs) as movable network nodes such as base stations and routers. In contrast, the node mobility of NTN introduces dynamic changes in the network topology, which decreases the opportunities and duration of NTN-ground communication. In addition, dynamic changes in the communication environment, such as weather, cause link quality and availability to fluctuate. Therefore, NTN brings challenges in keeping the packet delivery rate high due to its dynamic changes in topology and communication environment. This paper proposes a routing method with link information-based path calculation rule selection in NTN. The proposed method calculates paths according to the rules selected by the link information-based rule selection model using machine learning (ML). The rule selection model is trained with the dataset based on simulations of various training scenarios of an NTN. Simulation results for two evaluation scenarios demonstrate that the proposed method outperforms the existing routing methods in terms of packet delivery rate even under severe weather conditions. The results also show that each of the multiple path calculation rules contributes to increasing the packet delivery rate.

Index Terms—Routing, rule selection, non-terrestrial networks, machine learning, beyond 5G/6G.

I. INTRODUCTION

Future networks in beyond 5G/6G era are expected to provide ubiquitous connectivity to everywhere, including uncovered or underserved areas. In particular, the future networks will need to cover not only populated areas but also unpopulated areas such as ocean, air, and space. Therefore, a more efficient network infrastructure is essential to provide greater coverage instead of extending the existing terrestrial networks (TN) such as mobile and fixed networks. Hence, non-terrestrial networks (NTN) are becoming one of the most promising approaches to provide wider network connectivity from the sky. NTN employs satellites, high altitude platform stations (HAPS), and unmanned aerial vehicles (UAV) as flying network nodes, such as base stations and routers, in three-dimensional (3D) space.

While NTN is suitable for extending coverage, it also brings challenges in providing stable communication due to node mobility and dynamic environment such as weather. Node mobility in NTN makes the network topology dynamic with respect to time and introduces time limits during which NTN nodes can communicate with the ground nodes. Additionally, the dynamic environment causes link quality and connectivity

to fluctuate. In particular, a low earth orbit (LEO) satellite moves so fast (about seven kilometers per second) that an LEO satellite may only be visible from a ground station (GS) for about ten minutes. The availability of a link between an LEO satellite and a GS may vary depending on several factors such as weather, antenna directions, and inter-node distance. Hence, NTN brings challenges in keeping the packet delivery rate high due to its limited NTN-ground communication opportunities and intermittent link availability.

Routing is a fundamental process that selects an appropriate path from possible paths to deliver packets from a source node to a destination node. In particular, selecting appropriate paths for each moment considering node mobility and link availability becomes more critical in NTN. Existing routing methods, including routing protocols for mobile ad-hoc networks (MANET), are based on distributed routing, which exchanges messages in the network to detect topology changes and to calculate paths. While such distributed routing approaches provide versatility in applying to various networks, they have difficulties in finding optimal paths in NTN in terms of packet delivery rate as they cannot anticipate the dynamic changes in topology and environment such as weather. Additionally, the existing routing methods usually adopt the shortest path algorithm, an optimization algorithm that minimizes the sum of link cost (weight) for each possible path. However, such a path-finding mechanism might not be able to find a path that can deliver packets to the destination in NTN. For instance, the shortest path in terms of the number of hops from source to destination may suffer from rain loss in a heavy rain area, but another detour path, which is not the shortest path, may provide a higher packet delivery rate as it bypasses the rainy area. Therefore, another routing approach that selectively employs possible paths considering node mobility and link availability is necessary to keep the packet delivery rate high in NTN-ground communication.

This paper proposes a routing method with link information-based path calculation rule selection to increase the packet delivery rate in NTN. The proposed method calculates paths according to the rules selected by the link information-based rule selection model using machine learning (ML). The future link information is calculated based on orbital parameters and weather forecast data assuming that the future locations of NTN nodes can be predicted using orbital parameters, and the link quality can be calculated using propagation models such

as ITU-R rain loss model [1]. The rule selection model is trained with the dataset obtained by simulating different training scenarios of the NTN. Simulation results for evaluation scenarios demonstrate that the proposed method outperforms the existing routing methods in terms of packet delivery rate even under severe weather conditions. The results also show that each of the multiple path calculation rules contributes to increase the packet delivery rate.

The rest of this paper is organized as follows. Section II describes related work. Section III presents the proposed routing method. Section IV presents evaluation of the proposed method in terms of packet delivery rate in comparison with the existing methods. Finally, Section V concludes this paper.

II. RELATED WORK

Routing methods in dynamic networks have been presented in the field of ad-hoc networks. Ad-hoc On-Demand Distance Vector (AODV) [2] and Optimized Link State Routing (OLSR) [3] are two examples of routing protocols in MANET routing methods. In addition, modified versions of MANET routing methods have been presented in the literature [4], [5]. The work in [4] presented a modified version of AODV, where each node predicts link breakage and warns neighboring nodes when the link is about to break via control messages. The work in [5] presented a hello message interval control method using reinforcement learning to reduce bandwidth wastage due to frequent hello message flooding in flying ad-hoc networks (FANET). The hello message interval control method is incorporated into the existing MANET routing protocols, AODV and OLSR. The work in [6] presented an ML-based packet arrival rate prediction model to avoid high-traffic UAVs and minimize packet loss in UAV-based FANET. These existing routing methods are based on distributed routing, where dynamically changing network topology is continuously discovered by frequent control message flooding and path calculation is performed on the discovered topology. Although such routing methods have versatility in applying to various networks, they cannot anticipate the changes in dynamic network topology and environment such as weather. In addition, such routing methods are usually based on the shortest path algorithms, which may result in poor packet delivery rate in NTN as described in Section I. Our work presents a centralized routing method with path calculation rule selection from multiple rules using pre-calculated link information based on orbital parameters and weather forecast to improve packet delivery rate. Although the proposed method requires the pre-calculated link information, it is suitable for routing in dynamic networks such as NTN, whose node movement can be predicted.

Besides ad-hoc routing protocols, ML-based intelligent routing methods in dynamic networks have been presented in the literature [7]–[9]. The work in [7] presented a next hop selection model in ultra-low latency vehicular networks for autonomous driving. The work in [8] presented a deep reinforcement learning-based automatic path selection strategy. The work in [9] presented an ML-assisted routing optimization

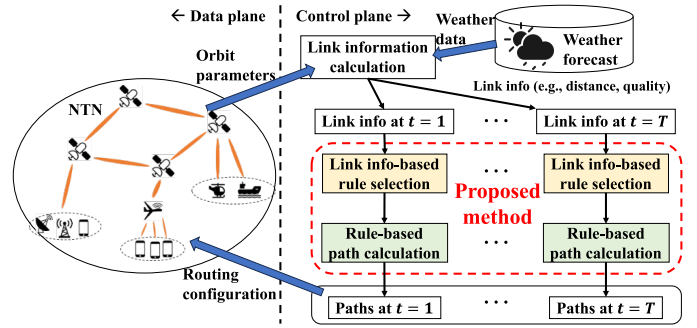


Fig. 1. Architecture for link information-based routing in NTN.

approach for energy-efficient communication in mobile networks. The ML-based path selection and next hop selection boils down to ML-based classification problems, where the number of labels increases with the size of the network. Our work differs from these approaches in selecting path calculation rules instead of selecting paths or next hops using ML technique, where the number of labels is constant and does not depend on the size of the network.

III. LINK INFORMATION-BASED ROUTING METHOD

A. Notation

An NTN during a given time period $t \in [1, T]$ is represented by a sequence of graphs $G = [g_1, \dots, g_T]$, since its topology and link information may change over time. Each graph in G has the set of links $\mathcal{L} = \{l_i | i \in [1, n_i]\}$, where \mathcal{L} is the common set for each graph in G . Each path between a source and a destination is defined as a sequence of links $p_k = [l_{k(1)}, \dots, l_{k(|p_k|)}] \in \mathcal{P}$, where $k(i)$ denotes the index of the i -th link in path p_k and \mathcal{P} is a set of possible paths in the NTN. The link information of l_i at time t is a set of features (properties) of link l_i , which is represented by a vector $\mathbf{x}_{l_i}(t) = [x_{l_i}^1(t), \dots, x_{l_i}^N(t)]$. N is the number of link features. A whole link information vector at time t is defined by $\mathbf{X}(t) = [\mathbf{x}_{l_1}(t), \dots, \mathbf{x}_{l_{n_t}}(t)]$. The link information at time t is embedded in the corresponding edges of graph g_t . A set of path calculation rules is represented by $\mathcal{R} = \{r | r \in [1, R]\}$. A link information-based rule selection function is denoted by $F_{(\mathcal{R}, s, d)}(\mathbf{X})$, where s and d are source and destination nodes, respectively. A function that calculates s -to- d path on graph g according to rule r is denoted by $F_r^P(g, s, d)$.

B. Architecture

We propose a routing method with link information-based rule selection in NTN. Fig. 1 presents an architecture for link information-based routing in NTN during a future time period $t \in [1, T]$. The architecture mainly consists of three functions: link information calculation, link information-based rule selection, and rule-based path calculation, where the proposed method consists of the latter two functions. The link information is a set of link features, such as propagation loss, propagation distance, bit error rate (BER), and other metrics. In the link information-based routing architecture,

Algorithm 1: Link information-based routing.

Input: G, s, d, \mathcal{R}
Output: $\mathbf{p}'(s, d)$
1 for $t \leftarrow 1$ to T do
2 $r'_t \leftarrow F_{(\mathcal{R},s,d)}(\mathbf{X}(t))$ // rule selection
3 $p'_t(s, d) \leftarrow F_{r'_t}^p(g_t, s, d)$ // path calculation
4 end
5 $\mathbf{p}'(s, d) \leftarrow [p'_1(s, d), \dots, p'_T(s, d)]$

the future link information is calculated in advance using the future locations of NTN nodes and the propagation loss considering the environment. We assume that future locations can be predicted using orbital parameters, such as two-line elements (TLEs), or flight paths of HAPS and UAVs planned in advance by network operators. The propagation loss considering environment is calculated using some propagation loss models, such as ITU-R P.618-12 rain loss model [1], taking as input the node locations and weather forecast data at each time t . The link information-based rule selection and rule-based path calculation are the main part of the architecture, which calculates paths according to the rules selected by the link information-based rule selection model for each time t . The link information-based rule selection function is an ML-based model that selects an appropriate path calculation rule based on the pre-calculated link information. Finally, a sequence of the selected paths during $t \in [1, T]$ is configured to the NTN, where packets from the source node are delivered to the destination node along with the configured paths.

Algorithm 1 describes the behavior of the proposed method. The proposed method takes as input a sequence of graph G containing link information for each link at each time $t \in [1, T]$, source s , destination d , and the set of path calculation rules \mathcal{R} . At each time $t \in [1, T]$, an appropriate path calculation rule r'_t is selected by $F_{(\mathcal{R},s,d)}$ based on the whole link information $\mathbf{X}(t)$. The rule selection function $F_{(\mathcal{R},s,d)}$ is an ML-based classification model that selects a path selection rule out of R rules taking $\mathbf{X}(t)$ as input. Then $F_{r'_t}^p$ calculates a s -to- d path $p'_t(s, d)$ according to the path calculation rule r'_t at time t . Finally, a sequence of calculated paths $\mathbf{p}'(s, d)$ is configured to the NTN.

C. Path calculation rules

Path calculation is a process of selecting the optimal path from possible sequences of links between a source and a destination in a network. A path calculation rule is an algorithm that outputs a path based on the input data. A well-known example of path calculation rule is the shortest path algorithm, which is represented as $\arg \min_{p_k \in \mathcal{P}} [\sum_{l_i \in p_k} c_i]$, where c_i is the cost (weight) of link l_i . The cost of each link may be set based on link information, represented as $c_i = f(x_j^{l_i})$ for $j \in [1, N]$, where f is an appropriate function. Hence, several different path calculation rules can be defined depending on the cost definition in the shortest path

Algorithm 2: Building process of rule selection model.

Input: $\mathcal{E}, \mathcal{R}, F^j, F^l$
Output: $F_{(\mathcal{R},s,d)}$
1 foreach $e \in \mathcal{E}$ do
2 $\mathbf{X}_e \leftarrow [\mathbf{X}_e(1), \dots, \mathbf{X}_e(T)]$
3 for $t \leftarrow 1$ to T do
4 for $r \leftarrow 1$ to R do
5 $\tilde{p}_{e,t,r}(s, d) \leftarrow F_r^p(g_{e,t}, s, d)$
6 $m_{e,t,r} \leftarrow F^j(e, \tilde{p}_{e,t,r}(s, d))$
7 end
8 $\mathbf{m}_{e,t} \leftarrow [m_{e,t,1}, \dots, m_{e,t,R}]$
9 $q_{e,t} \leftarrow F^l(\mathbf{m}_{e,t})$
10 end
11 $\mathbf{q}_e \leftarrow [q_{e,1}, \dots, q_{e,T}]$
12 end
13 $\mathcal{D} \leftarrow [(\mathbf{X}_1, \mathbf{q}_1), \dots, (\mathbf{X}_E, \mathbf{q}_E)]$
14 $F_{(\mathcal{R},s,d)} \leftarrow \text{train}(\mathcal{D})$

algorithm. Besides the shortest path-based rules, other path calculation rules can be considered. Let x_i denote E_b/N_0 , energy per bit to noise power spectral density ratio, of link l_i in path p_k , $\arg \max_{p_k \in \mathcal{P}} [\min_{l_i \in p_k} x_i]$ is a rule that selects the path with the largest minimum E_b/N_0 value for each link comprising the path in the network. Note that the path calculation rules included in the proposed method are not limited to any particular ones.

D. Path calculation rule selection model and training dataset

The path calculation rule selection function $F_{(\mathcal{R},s,d)}$ is an ML model of R -class classification based on supervised learning. Algorithm 2 describes the building process of $F_{(\mathcal{R},s,d)}$ including the dataset generation process. The training of $F_{(\mathcal{R},s,d)}$ is based on a dataset \mathcal{D} , whose input data is link information and output label is a path calculation rule at each time t . The path calculation rule selection model $F_{(\mathcal{R},s,d)}$ is trained using the dataset \mathcal{D} in line 14. Note that training method of $F_{(\mathcal{R},s,d)}$ is not restricted to any particular one in this work.

We consider a set of NTN scenarios, represented by a set $\mathcal{E} = \{e | e \in [1, E]\}$, to obtain the dataset \mathcal{D} . Each scenario e defines G_e, s, d , and some other parameters such as each antenna direction and weather condition. Table I describes the qualitative link information for five example cases with different antenna directions and weather conditions. In cases (a) and (b), the antennas of satellites and GSs face each other with good weather conditions, which provides high SNR and low BER. Case (a) likely to provide better link quality than case (b) because the propagation distance in case (a) is shorter than in case (b). In case (c), the satellite antenna does not face the GS antenna, which results in low SNR and high BER while the distance is not long. In cases (d) and (e), while the antennas of satellites and GSs face each other, there is rainfall, which degrades signal power, resulting in low SNR and high BER. Likewise cases (a) and (b), case (e) may lead

TABLE I
EXAMPLES OF LINK INFORMATION VARIATIONS FOR DIFFERENT SCENARIO PARAMETERS.

Example cases with different antenna directions and weather conditions	(a)	(b)	(c)	(d)	(e)
SNR	High	High	Low	Low	Low
Distance	Short	Long	Short	Short	Long
BER	Low	Low	High	High	High

to poor link quality because its propagation distance is long in addition to the rainfall. Thus, antenna directions and weather conditions differentiate each scenario in terms of link quality and availability. Therefore, running multiple scenarios, each with different conditions, produces a dataset with different link information and path calculation rule labels. Note that the quantitative link information is obtained and is used to train the rule selection model in the proposed method, while Table I presents a qualitative analysis for simplicity.

In Algorithm 2, lines 1 through 13 represent the dataset building process. Line 6 represents the packet delivery judgment process that judges whether a packet is delivered to the destination along with a path calculated by a rule. In particular, a function $F^j(e, \tilde{p}_{e,t,r}(s, d))$ judges whether a packet from s is successfully delivered to d along with the path $\tilde{p}_{e,t,r}$, where $\tilde{p}_{e,t,r}$ is the path calculated according to rule r at time t in scenario e . The judgment result is stored in $m_{e,t,r}$, where $m_{e,t,r}$ is set to 1 if a packet from s is delivered to d along a path $\tilde{p}_{e,t,r}(s, d)$, and is set to 0 otherwise. In practice, F^j may be some simulators, where we use a network simulator EXata [10] in Section IV. In line 9, a function F^l decides a label of path calculation rule based on the judgment result $m_{e,t}$. $m_{e,t}$ is an R -element vector containing binary results at time t in scenario e for rule $r \in [1, R]$ at r -th element. For instance, $\min \left[\arg \max_{r \in \mathcal{R}} (m_{e,t}) \right]$ selects as the label $q_{e,t}$ at time t in scenario e the minimum path calculation rule index r whose delivery result $m_{e,t,r}$ is 1. Finally, a sequence of link information and labeled rule pair for each scenario e is stored as dataset \mathcal{D} .

IV. EVALUATION

We evaluate the packet delivery rate of the proposed routing method on an example NTN in comparison with two existing routing methods, AODV [2] and OLSR [3].

A. Example NTN

We consider an example NTN consisting of a group of LEO satellites, GSs, and a data center (DC) as shown in Fig. 2. The LEO satellites, denoted as Sat 1, 2, 3, 4, 5, and 6, move from the west to the east passing over Japan. Each satellite

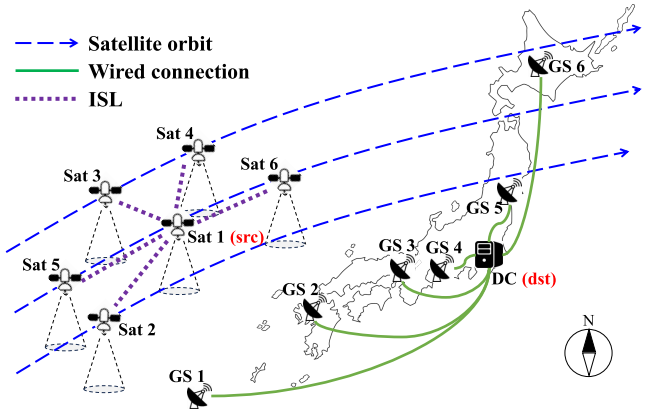


Fig. 2. Example NTN. A group of six LEO satellites pass over Japan. Six GSs are geographically distributed and connected to DC. Sat 1 is the source and the DC is the destination. Packet delivery rate of the proposed method and the existing methods are evaluated in the example NTN.

has an antenna to communicate with the GSs. Sat 1 is also connected to the other satellites via inter-satellite links (ISLs) for inter-satellite communication. Six GSs, denoted as GS 1, 2, 3, 4, 5, and 6, are geographically distributed throughout Japan. The DC located at Tokyo is connected to each of the GSs via terrestrial networks. Sat 1 is the source of the traffic that sends data to the DC as the satellites pass over Japan. Traffic from Sat 1 may be routed directly to the DC via one of the six GSs, or may be routed along with detour paths via other satellites and GSs if necessary. For instance, a path [Sat 1 – GS 4 – DC] may be used if the weather permits, but a detour path [Sat 1 – Sat 5 – GS 2 – DC] may be used if there is a heavily rained area around some GSs.

B. Link information and path calculation rules in evaluation

We describe the features of link information, path calculation rules, training scenarios to build the dataset and to train the rule selection model, and evaluation scenarios to evaluate the packet delivery rate of the proposed routing methods in this work. In this evaluation, link information is calculated for each inter-satellite link and satellite-GS link by using the Systems Tool Kit (STK) [11] from Analytical Graphic Inc. (AGI). We used eight features for each link; Equivalent Isotropic Radiation Power (EIRP), propagation loss, G/T, E_b/N_0 , BER, distance, and two additional features. One of the additional features is a bit that represents the link availability determined by STK. The other one is a bit that represents whether the link is an ISL or a satellite-GS link.

We consider four path calculation rules in this evaluation, denoted as rule 1, 2, 3, and 4; rule 1 is to select the path with the largest minimum E_b/N_0 value for each link comprising the path, rule 2 is to select the path with the largest total E_b/N_0 value for the path, rule 3 is to select the path with the smallest sum of the distance values of the paths, and rule 4 is to select the path with the smallest maximum BER value for each link comprising the path.

C. Scenarios for training and evaluation

We consider 35 training scenarios of the example NTN during time period $1 \leq t \leq 600$ [s]. Each of the training scenarios differs from the others in the directions of the antennas of the satellites and the antennas of the GSs so that the training dataset contains different link information and labels. For instance, one training scenario has a setting in which the antenna of Sat 6, the antennas of the other satellites, and the antennas of all the GSs are pointed at GS 3, vertically downward, and at Sat 6, respectively. All the training scenarios are in good weather conditions with no rainy areas. According to Algorithm 2, the training labels of the path calculation rule are obtained as a result of F^j for each rule r at each time t in each training scenario e , which constitute the training dataset \mathcal{D} . We obtained 11692, 10571, 1247, and 724 data for rule 1, 2, 3, and 4, respectively, which are finally randomly under-sampled to 2896 data in total. We trained the rule selection model $F_{(\mathcal{R},s,d)}$ based on the dataset using the random forest algorithm in scikit-learn [12] with its default parameters, whose accuracy score reaches 0.92. Note that the evaluation metric in this work is the packet delivery rate, where the accuracy score of the training is only for reference.

We also consider two different evaluation scenarios. Both evaluation scenarios have a heavy rain area in the central region of Japan and have an antenna setting in which all the satellites' antennas point straight down. All the GSs' antenna are pointed to Sat 4 and to Sat 5 in the evaluation scenario 1 and 2, respectively. In particular, all the GSs are more likely to be connected to Sat 4 and to Sat 5 via high quality links than to other satellites in the evaluation scenario 1 and 2, respectively. Fig. 3 shows the evaluation scenario 2 during the time period $t \in [1, 600]$ in three parts, where each part corresponds to every 200 seconds of the scenario. In part 1, Sat 1 can communicate with GSs in the western part, such as GS 1 or GS 2, directly or via Sat 5 as satellites are far from the rainy area. In part 2, while Sat 1 cannot communicate directly with GSs as Sat 1 reaches over the rainy area, Sat 1 can still communicate with GS 1 or GS 2 via Sat 5. In part 3, most of the satellites have passed over the rainy area and are in the eastern area. Hence, the paths from Sat 1 to the DC via high quality links change from those in part 1 and 2. Therefore, routing methods become critical to keep the delivery rate high in each part of the scenario. In the evaluation scenario, paths can be calculated at each time according to the selected rule by the rule selection model trained based on the training scenario. Note that the two evaluation scenarios are not included in the training scenarios, where all the training scenarios do not contain rainy areas.

Each scenario is run on the simulation system, which consists of Analytical Graphic Inc. (AGI)'s Systems Tool Kit (STK) [11] Pro version 12.3 and Keysight's EXata [10] version 7.3.2.0. We import real weather data on August 13, 2021, when a strong typhoon hit Japan, from the Japan Meteorological Agency [13]. The weather data are in the network common data form (netCDF) format, which records

TABLE II
SIMULATION RESULTS OF DELIVERY RATE FOR EACH 200 SEC PART FOR DIFFERENT ROUTING METHODS IN EVALUATION SCENARIOS 1 AND 2.

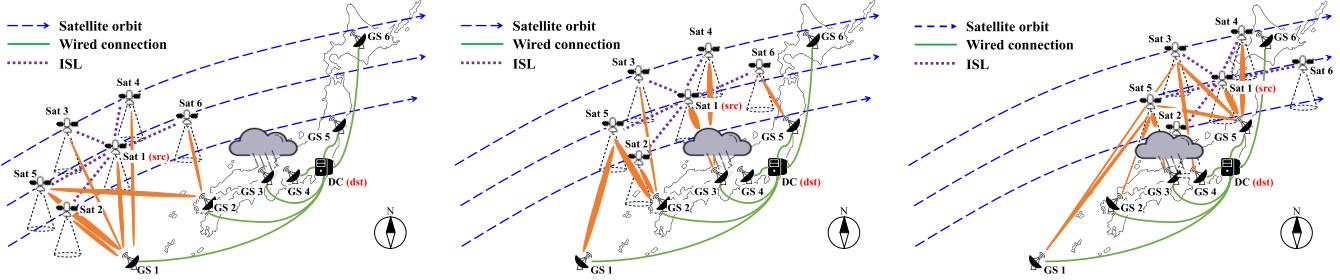
Example scenario 1	Sent packets	Delivered packets (Delivery rate)		
		Proposed	AODV	OLSR
Part 1	20,000	18,528 (0.93)	19,984 (0.99)	18,093 (0.90)
Part 2	20,000	18,689 (0.93)	19,641 (0.98)	15,660 (0.78)
Part 3	20,000	18,552 (0.93)	670 (0.03)	8,131 (0.41)
Total	60,000	55,769 (0.93)	40,295 (0.67)	41,884 (0.70)
Example scenario 2	Sent packets	Delivered packets (Delivery rate)		
		Proposed	AODV	OLSR
Part 1	20,000	18,517 (0.93)	19,978 (0.99)	18,217 (0.91)
Part 2	20,000	17,614 (0.88)	19,984 (0.99)	15,575 (0.78)
Part 3	20,000	17,948 (0.90)	7,196 (0.36)	9,870 (0.49)
Total	60,000	54,079 (0.90)	47,158 (0.79)	43,662 (0.73)

the weather data for each geographical location and time. The rain loss of the satellite-GS links is calculated by using the ITU-R P.618-12 rain loss model [1] for each geographical location and time. We consider constant bit rate (CBR) traffic from Sat 1 to DC, consisting of 512-byte user datagram protocol (UDP) packets at a rate of 100 packets per second for 600 seconds.

D. Simulation results

Table II shows the simulation results of the packet delivery rate for three different routing methods in the evaluation scenarios 1 and 2. In both evaluation scenarios, the proposed method outperforms the existing routing methods in terms of the number of delivered packets and the packet delivery rate. This is because the proposed method is based on the pre-calculated link information and leverages multiple path calculation rules selectively at each moment whereas the existing methods calculate the shortest paths on the discovered topology even if the link quality of the shortest path is poor. In addition, the topology discovery of the existing method is based only on the control message flooding, where detailed link information that incorporates rain loss due to weather data cannot be used.

While both existing methods show almost the same packet delivery rate for the entire scenario, OLSR works better than AODV in part 3 for both example scenarios. This is due to the difference between the two routing protocols. Since AODV is a reactive routing protocol, its path calculation starts only when the source starts communicating. AODV basically calculates paths only when a source-to-destination path is unavailable or broken links are detected on the active path, which is based on message flooding. Therefore, AODV tends to continue using the active paths when they are available. In contrast, OLSR is a proactive routing protocol that periodically floods messages to discover the topology, where the shortest paths are calculated on the discovered topology. As a result, OLSR tends to change active paths based on detected topology changes. Therefore, OLSR has more chances to change the active paths to keep



(a) Part 1 of evaluation scenario 2, $t \in [1, 200]$. (b) Part 2 of evaluation scenario 2, $t \in [200, 400]$. (c) Part 3 of evaluation scenario 2, $t \in [400, 600]$.

Fig. 3. Images of evaluation scenario 2 in three parts during time period $t \in [1, 600]$. There is a typhoon with heavy rain in the central region of Japan. All the satellites's antenna point to straight down and all the GSs are targeted to Sat 5.

TABLE III
NUMBERS OF DELIVERED PACKETS FOR EACH PATH CALCULATION RULE
IN EACH EVALUATION SCENARIO.

	Rule 1	Rule 2	Rule 3	Rule 4
Evaluation scenario 1	20668	23830	4305	152
Evaluation scenario 2	34195	18762	1122	0

up with the topology changes in part 3 compared to AODV, which may result in OLSR's higher packet delivery rate in part 3.

In addition, while AODV slightly outperforms the proposed method in parts 1 and 2, the proposed method significantly outperforms AODV in part 3. We consider that this is because of the prediction error of the rule selection model in the proposed method. In particular, less than 10 % of the packets are routed along with paths calculated by wrong rules because the accuracy of the rule selection model $F(\mathcal{R}, s, d)$ is about 92 % and not 100 %. However, the proposed method keeps the packet delivery rate constant even in part 3, which enables stable communication compared to the existing methods.

The numbers of delivered packets for each path calculation rule in each evaluation scenario are presented in Table III. While the numbers vary by rule and scenario, each of the rules introduced in this evaluation contributes to the packet delivery rate. In particular, rules 1 and 2 are E_b/N_0 -based rules, which contribute to delivering most of the delivered packets, whereas distance-based rule 3 and BER-based rule 4 also contribute to the other delivered packets. Therefore, the proposed method selectively leverages the multiple rules to keep the packet delivery rate high in each part in each evaluation scenario.

V. CONCLUSION

This paper proposed a routing method with link information-based path calculation rule selection in NTN. The proposed method consists of two components; one is the path calculation rule selection based on link information, and the other is the path calculation according to the selected rule. While the proposed method requires pre-calculated link information of the NTN, it enables path calculation using multiple rules to increase the packet delivery rate in dynamic

networks. The path calculation rule selection model is trained based on the training scenarios of an example NTN. The proposed method is evaluated in terms of packet delivery rate in evaluation scenarios of the example NTN. The simulation results demonstrated that the proposed method outperforms the existing routing methods in two evaluation scenarios. In particular, the proposed method keeps the packet delivery rate high compared to the existing methods even under dynamic changes in topology and link availability due to severe weather. The results also show that each of the multiple path calculation rules contributes to increasing the packet delivery rate, where selectively using multiple rules finds valid paths to deliver more packets.

REFERENCES

- [1] "Recommendation ITU-R P.618-12 Propagation data and prediction methods required for the design of Earth-space telecommunication systems," 2015.
- [2] S. R. Das, C. E. Perkins, and E. M. Belding-Royer, "Ad hoc On-Demand Distance Vector (AODV) Routing," RFC 3561, Jul. 2003.
- [3] T. H. Clausen and P. Jacquet, "Optimized Link State Routing Protocol (OLSR)," RFC 3626, Oct. 2003.
- [4] A. Yadav, Y. N. Singh, and R. R. Singh, "Improving Routing Performance in AODV with Link Prediction in Mobile Adhoc Networks," *Wireless Pers. Commun.*, vol. 83, no. 1, pp. 603–618, Jul. 2015.
- [5] M. S. Ayub, P. Adasme, D. C. Melgarejo, R. L. Rosa, and D. Z. Rodríguez, "Intelligent Hello Dissemination Model for FANET Routing Protocols," *IEEE Access*, vol. 10, pp. 46 513–46 525, 2022.
- [6] M. Zhang, C. Dong, P. Yang, T. Tao, Q. Wu, and T. Q. S. Quek, "Adaptive Routing Design for Flying Ad Hoc Networks," *IEEE Commun. Lett.*, vol. 26, no. 6, pp. 1438–1442, Jun. 2022.
- [7] Q. Meng, J. Wei, X. Wang, and H. Guo, "Intelligent Routing Orchestration for Ultra-Low Latency Transport Networks," *IEEE Access*, vol. 8, pp. 128 324–128 336, 2020.
- [8] P. Sun, Y. Hu, J. Lan, L. Tian, and M. Chen, "TIDE: Time-relevant deep reinforcement learning for routing optimization," *Future Gener. Comput. Syst.*, vol. 99, pp. 401–409, 2019.
- [9] D. Jiang, Z. Wang, W. Wang, Z. Lv, and K.-K. R. Choo, "AI-Assisted Energy-Efficient and Intelligent Routing for Reconfigurable Wireless Networks," *IEEE Trans. Netw. Sci. Eng.*, vol. 9, no. 1, pp. 78–88, 2022.
- [10] "EXata." [Online]. Available: <https://www.keysight.com>
- [11] "Systems Tool Kit (STK)." [Online]. Available: <https://www.agi.com>
- [12] F. Pedregosa, G. Varoquaux, A. Gramfort, V. Michel, B. Thirion, O. Grisel, M. Blondel, P. Prettenhofer, R. Weiss, V. Dubourg, J. Vanderplas, A. Passos, D. Cournapeau, M. Brucher, M. Perrot, and E. Duchesnay, "Scikit-learn: Machine learning in Python," *J. Mach. Learn. Res.*, vol. 12, pp. 2825–2830, 2011.
- [13] "Weather data in netCDF taken from the Japan Meteorological Agency." [Online]. Available: <http://database.rish.kyoto-u.ac.jp/arch/jmadata/data/gpv/netcdf/>